

Provided for non-commercial research and education use.
Not for reproduction, distribution or commercial use.



(This is a sample cover image for this issue. The actual cover is not yet available at this time.)

This article appeared in a journal published by Elsevier. The attached copy is furnished to the author for internal non-commercial research and education use, including for instruction at the authors institution and sharing with colleagues.

Other uses, including reproduction and distribution, or selling or licensing copies, or posting to personal, institutional or third party websites are prohibited.

In most cases authors are permitted to post their version of the article (e.g. in Word or Tex form) to their personal website or institutional repository. Authors requiring further information regarding Elsevier's archiving and manuscript policies are encouraged to visit:

<http://www.elsevier.com/copyright>



Contents lists available at SciVerse ScienceDirect

Earth and Planetary Science Letters

journal homepage: www.elsevier.com/locate/epslSpin crossover of iron in aluminous MgSiO₃ perovskite and post-perovskite

Han Hsu*, Yonggang G. Yu, Renata M. Wentzcovitch

Department of Chemical Engineering and Materials Science, University of Minnesota, Minneapolis, MN 55455, USA

ARTICLE INFO

Article history:

Received 30 May 2012

Received in revised form

17 September 2012

Accepted 19 September 2012

Editor: L. Stixrude

Keywords:

spin crossover
quadrupole splitting
perovskite
post-perovskite
lower mantle
first-principles

ABSTRACT

Using density functional theory+Hubbard U (DFT+ U) calculations, we investigate how aluminum affects the spin crossover of iron in MgSiO₃ perovskite (Pv) and post-perovskite (Ppv), the major mineral phases in the Earth's lower mantle. We find that the presence of aluminum does not change the response of iron spin state to pressure: only ferric iron (Fe³⁺) in the octahedral (B)-site undergoes a crossover from high-spin (HS) to low-spin (LS) state, while Fe³⁺ in the dodecahedral (A)-site remains in the HS state, same as in Al-free cases. However, aluminum does significantly affect the placement of Fe³⁺ in these mineral phases. The most stable atomic configuration has all Al³⁺ in the B -site and all Fe³⁺ in the A -site (thus in the HS state). Metastable configurations with LS Fe³⁺ in the B -site can happen only at high pressures and high temperatures. Therefore, experimental observations of LS Fe³⁺ at high pressures in Al-bearing Pv require diffusion of iron from the A -site to the B -site and should be sensitive to the annealing temperature and schedule. In the Earth's lower mantle, the elastic anomalies accompanying the B -site HS-LS crossover exhibited in Al-free Pv are likely to be considerably reduced, according to the B -site Fe³⁺ population.

© 2012 Elsevier B.V. All rights reserved.

1. Introduction

Pressure-induced spin crossovers of iron in Earth minerals have attracted great attention since the discovery of this phenomenon (Badro et al., 2003, 2004). As well studied in ferropervicase (the second most abundant mineral in the Earth's lower mantle), spin crossover can produce elastic, thermodynamic, optical, and conducting anomalies in the host minerals (Crowhurst et al., 2008; Goncharov et al., 2006; Hsu et al., 2010c; Lin et al., 2005, 2007a, 2007b; Tsuchiya et al., 2006; Wentzcovitch et al., 2009; Wu et al., 2009). While the geophysical consequences of these anomalies have been anticipated, further investigations are still necessary. In contrast to ferropervicase, spin crossovers in magnesium silicate (MgSiO₃), perovskite (Pv), and post-perovskite (Ppv), the major mineral phases in the lower mantle, have been controversial for years. One reason for such controversy is the complicated nature of these minerals. In Pv and Ppv, ferrous iron (Fe²⁺) and ferric iron (Fe³⁺) coexist, and they both have three possible spin states: high-spin (HS), intermediate-spin (IS), and low-spin (LS). In addition, Fe³⁺ can occupy the dodecahedral (A)-site and the octahedral (B)-site (Fe²⁺ only occupies the A -site), so there can be up to nine possible states to be considered. Another reason for this iron-spin controversy is the lack of definitive tools to directly identify the iron spin

* Corresponding author. Current address: Department of Physics, National Central University, Jhongli City, Taoyuan 32001, Taiwan.
Tel.: +886 3 422 7151x65303.

E-mail address: hanhsu@ncu.edu.tw (H. Hsu).

state and occupying site. Indeed, x-ray emission spectroscopy (XES) and Mössbauer spectroscopy have been widely used, but their interpretations can be ambiguous. For example, decreases of the satellite peak ($K\beta'$) intensity observed in XES spectra of Pv containing both Fe²⁺ and Fe³⁺ were interpreted in terms of HS-IS or HS-LS crossover of Fe²⁺ (Badro et al., 2004; Li et al., 2004; McCammon et al., 2008), but a highly similar $K\beta'$ decrease was also observed in Pv containing only Fe³⁺ (Catalli et al., 2010b). Clearly, while the decrease of $K\beta'$ intensity is a signature of the decrease of average electron spin moment of iron in Pv, extracting the detailed spin-crossover mechanism in such a complicated system solely based on XES spectra is extremely difficult. Interpretation of Mössbauer spectra without other information can be ambiguous as well. A sudden increase in the nuclear quadrupole splitting (QS) of Fe²⁺ (from 2.4 to 3.5 mm/s) in Pv has been interpreted in terms of HS-IS or HS-LS crossover (Jackson et al., 2005; Li et al., 2006; McCammon et al., 2008). To understand spin crossover in Pv and to explain the above experimental observations, plenty of calculations have been conducted (Bengtson et al., 2008; Hofmeister, 2006; Stackhouse et al., 2007; Umemoto et al., 2008, 2009; Zhang and Oganov, 2006), but consistency with experiments was not achieved until recently (Bengtson et al., 2009; Catalli et al., 2010b; Hsu et al., 2010b, 2011; Lin et al., 2012). It turns out that Fe²⁺ in Pv does not undergo a spin crossover; it remains in the HS state throughout the lower-mantle pressure range (23–135 GPa) with a change in orbital occupancy (and thus QS) occurring at about 20–30 GPa (Hsu et al., 2010b). It is the B -site Fe³⁺ in (Mg,Fe)(Si,Fe)O₃ Pv going through a HS-LS crossover at 50–60 GPa, which is accompanied by a volume reduction

and suggests a possible source of seismic anomalies (Catalli et al., 2010b; Hsu et al., 2011). As to Ppv, a high QS (3.5–4.0 mm/s) of Fe^{2+} was interpreted as a signature of the IS state (Lin et al., 2008; Mao et al., 2010). However, first-principles calculations have shown it to be the HS state (Yu et al., 2012). Yu et al. (2012) have also shown that for Al-free Ppv in the D'' pressure range (120–135 GPa), the A- and B-sites Fe^{3+} are in the HS and LS state, respectively, and the calculated QSs of these two states are consistent with Mössbauer spectra (Catalli et al., 2010a; Jackson et al., 2009; Mao et al., 2010).

The success of first-principles calculations in studying Fe-bearing minerals mainly results from the development of density function theory + Hubbard U (DFT+ U) method [see Cococcioni, 2010 for a comprehensive review]. In contrast to standard DFT methods, such as local density approximation (LDA) or generalized gradient approximation (GGA), the on-site Coulomb interaction of iron is more accurately treated by including the Hubbard U correction. With this correction, states inaccessible in standard DFT calculations can be obtained, such as the two HS Fe^{2+} with distinct QSs and the B-site HS Fe^{3+} in Pv and Ppv (Hsu et al., 2010b, 2011; Yu et al., 2012). In particular, when the Hubbard U parameters are computed self-consistently by first principles (referred to as U_{sc} , see Section 2), the predicted transition pressure is in good agreement with experiments (Hsu et al., 2011). So far, the DFT+ U_{sc} method has been applied to Al-free Pv/Ppv. With a small fraction of Al_2O_3 known to be accommodated in Pv in the lower-mantle condition (Frost et al., 2004; Irifune, 1997; Kesson et al., 1998; McCammon, 1997), Al-bearing Pv/Ppv is believed to be more important in the lower mantle. However, these mineral phases have been computationally studied via standard DFT methods only (Caracas, 2010; Li et al., 2005; Zhang and Oganov, 2006), and standard DFT calculations cannot fully explain the contradictive experimental results described below. Using Mössbauer spectroscopy, Li et al. (2006) did not observe any crossover in Al-bearing Pv in 0–100 GPa, but Catalli et al. (2011) showed a fraction of Fe^{3+} undergoes a crossover from QS ~ 1 mm/s to QS ~ 2.1 mm/s when $P > 80$ GPa, along with a decrease in the $K\beta'$ intensity, which was also reported by Fujino et al. (2012). Furthermore, the transition pressure observed in Al-bearing Pv (Catalli et al., 2011) is significantly higher than that in Al-free Pv (Catalli et al., 2010b). This finding strongly suggests that changes of iron spin state in these two systems may have different mechanisms. To properly address iron spin problems in complicated systems like Al-bearing Pv/Ppv, detailed and carefully conducted DFT+ U_{sc} calculations are thus highly desirable, given their previous success in Al-free cases.

2. Computation details

In this paper, we performed structural optimization for 40-atom supercells of Fe- and Al-bearing Pv/Ppv (Fig. 1) using variable cell shape molecular dynamics (Wentzcovitch et al., 1993) implemented in the QUANTUM ESPRESSO code (Giannozzi et al., 2009), in which the plane-wave pseudopotential method is adopted. Pseudopotentials used in this paper have been reported by Umemoto et al. (2008), with a plane-wave energy cutoff of 40 Ry. In our calculations for Al-bearing Pv/Ppv, we find metastable IS Fe^{3+} in both the A- and B-sites, in contrast to the Al-free cases where IS Fe^{3+} was only found in the A-site. We used a linear response approach (Cococcioni and de Gironcoli, 2005) to compute spin-dependent U_{sc} 's until self consistency is achieved (Hsu et al., 2011; Kulik et al., 2006). The U_{sc} 's of the newly found B-site IS Fe^{3+} are 4.1 and 4.2 eV for Pv and Ppv, respectively. The U_{sc} 's of other states are the same as the Al-free cases; their numerical values have been reported previously (Hsu et al., 2011;

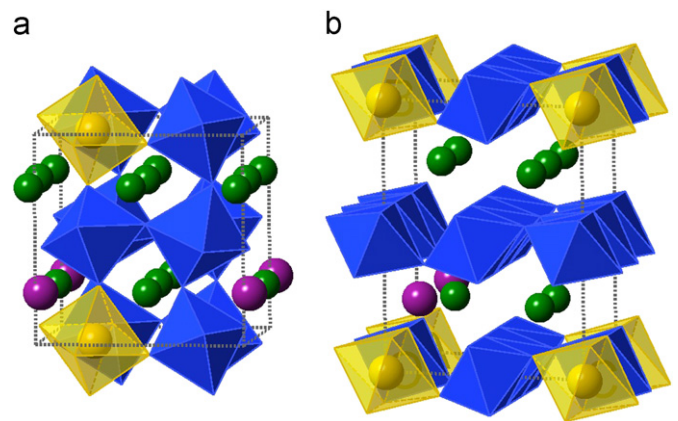


Fig. 1. Atomic structure of Fe- and Al-bearing MgSiO_3 perovskite (a) and post-perovskite (b), where the 40-atom supercells are indicated by the dotted lines. Green spheres and blue octahedra indicate Mg and SiO_6 octahedra, respectively. Purple and yellow spheres indicate substituting atoms at the A- and B-sites, respectively. (For interpretation of the references to color in this figure caption, the reader is referred to the web version of this article.)

Yu et al., 2012). The volume dependence of these U_{sc} 's is negligible. To be more rigorous, the Hubbard U mentioned in this paper is effectively the $U-J$ introduced by Dudarev et al. (1998). The electric field gradient (EFG) tensors are computed using the WIEN2k code (Blaha et al., 2001), in which the augmented plane-wave plus local orbitals (APW+lo) method (Madsen et al., 2001) is implemented. The EFGs were converted to QSs with the ^{57}Fe nuclear quadrupole moment $Q=0.16$ (Pettrilli et al., 1998) and 0.18 barn for the possible uncertainty. A shifted $4 \times 4 \times 4$ \mathbf{k} -point grid was used to calculate the EFG, while a $2 \times 2 \times 2$ and a $4 \times 4 \times 4$ grids produce the same atomic structure.

3. Results and discussion

3.1. Fe- and Al-bearing MgSiO_3 perovskite

In Pv, Fe^{3+} can substitute Mg or Si in the A- or B-site, respectively. To understand how the iron spin state responds to pressure in these two non-equivalent sites, we first consider the coupled substitutions of Fe^{3+} and Al^{3+} in a 40-atom supercell, forming $(\text{Mg}_{1-x}\text{Fe}_x)(\text{Si}_{1-x}\text{Al}_x)\text{O}_3$ or $(\text{Mg}_{1-x}\text{Al}_x)(\text{Si}_{1-x}\text{Fe}_x)\text{O}_3$ Pv ($x=0.125$), with Fe^{3+} and Al^{3+} occupying nearest A- and B-sites [Fig. 1(a)]. For each configuration, relative enthalpies (ΔH) of all possible spin states (HS, IS, and LS) are computed using LDA+ U_{sc} and GGA+ U_{sc} [PBE-type GGA Perdew et al., 1996], as shown in Fig. 2. The results are very similar to that of Al-free Pv (Hsu et al., 2011): the A-site Fe^{3+} remains in the HS state in 0–150 GPa [Fig. 2(a) and (b)], and the B-site Fe^{3+} undergoes a HS-LS crossover [Fig. 2(c) and (d)] at a transition pressure $P_T \sim 43$ GPa in LDA+ U_{sc} and $P_T \sim 70$ GPa in GGA+ U_{sc} . Since LDA+ U_{sc} predicts more accurate equation of state and transition pressure (Hsu et al., 2011), we only present LDA+ U_{sc} calculations hereafter. The computed QSs of these states are shown in Fig. 2(e), along with those extracted from Mössbauer spectra (Catalli et al., 2011; Li et al., 2006), shown in Fig. 2(f). For the newly found B-site IS Fe^{3+} , the EFGs at various pressures are computed. The QS plotted in Fig. 2(e) ranges from the lowest to the highest QS we obtained for this particular state. For the other states, we did not compute their EFGs at every pressure. We tested a few cases and noticed that they are essentially the same as those in Al-free Pv and are in excellent agreement with the measured QS shown in Fig. 2(f). Here, we simply adopt previous Al-free calculation results (Hsu et al., 2011) for these states. Noticeable in Fig. 2(e), the

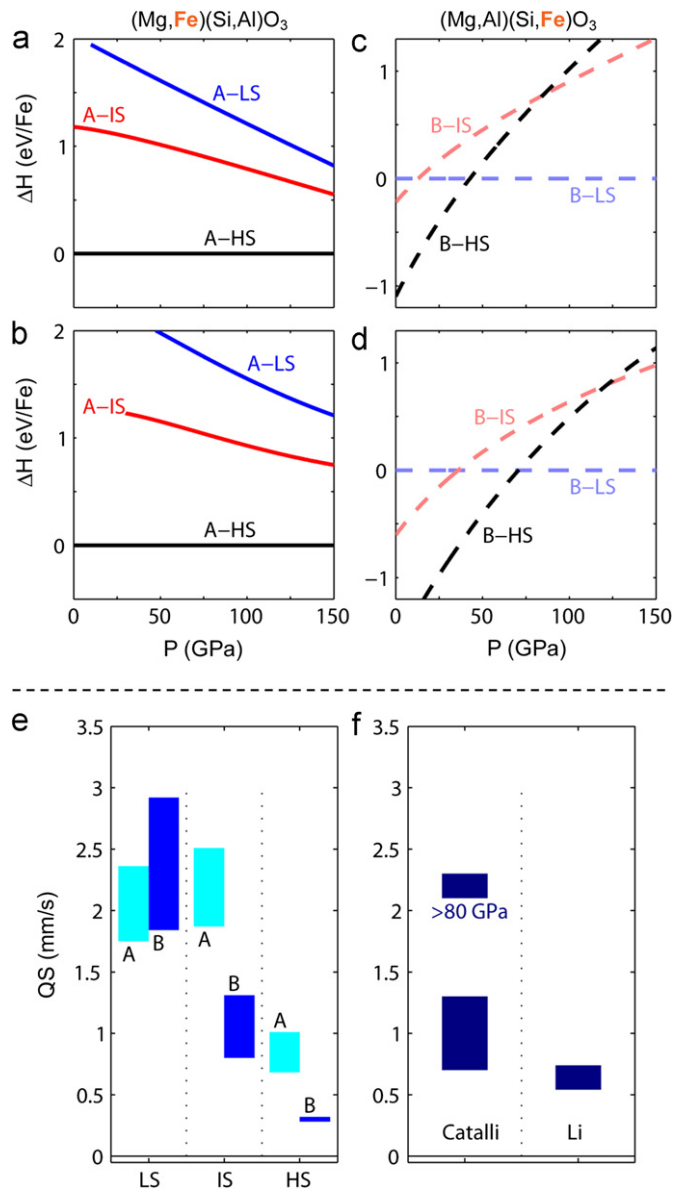


Fig. 2. Relative enthalpies and quadrupole splittings of Al-bearing Pv in different spin states. (a) and (b) Relative enthalpies of A-site Fe^{3+} in $(\text{Mg,Fe})(\text{Si,Al})\text{O}_3$ determined with LDA+ U_{sc} and GGA+ U_{sc} . (c) and (d) Relative enthalpies of B-site Fe^{3+} in $(\text{Mg,Al})(\text{Si,Fe})\text{O}_3$ determined with LDA+ U_{sc} and GGA+ U_{sc} . (e) Computed QSs of A- and B-sites Fe^{3+} using LDA+ U_{sc} (the QS of B-site IS Fe^{3+} is newly computed, the others are adopted from Hsu et al., 2011). (f) QS of Fe^{3+} extracted from Mössbauer spectra of Al-bearing Pv (Catalli et al., 2011; Li et al., 2006).

computed QS of the B-site IS Fe^{3+} is in between those of LS and HS Fe^{3+} . This trend is similar to that of the A-site Fe^{2+} and Fe^{3+} in Al-free Pv/Ppv and that of Co^{3+} in bulk and thin-film LaCoO_3 (Hsu et al., 2010a, 2010b, 2011, 2012; Yu et al., 2012). By comparing the QS and relative enthalpy of each spin state, the QS of about 2.1 mm/s observed by Catalli et al. (2011) at $P > 80$ GPa is most likely a signature of B-site LS Fe^{3+} . A question arises then: why was the B-site LS Fe^{3+} not observed at lower pressures (50–60 GPa) as in Al-free Pv (Catalli et al., 2010b), and why was it not observed by Li et al. (2006), as indicated in Fig. 2(f)?

To thoroughly understand site occupancies and spin states of iron in high pressure experiments or in the lower mantle, investigation of real solid solutions should be conducted. Such a task, however, is beyond the scope of this paper. Here, we give the first steps towards this investigation and insightful results that

can help to interpret experimental observations. We considered three qualitatively different atomic configurations: $(\text{Mg,Fe})(\text{Si,Al})\text{O}_3$, $(\text{Mg,Al})(\text{Si,Fe})\text{O}_3$, and a mixture of $(\text{Mg,Fe})(\text{Si,Fe})\text{O}_3$ and $(\text{Mg,Al})(\text{Si,Al})\text{O}_3$ Pv, with Fe–Fe and Al–Al pairs occupying the nearest A- and B-sites. Separated pairs (Al–Fe, Al–Al, or Fe–Fe pairs not occupying the nearest A- and B-sites) may occur, but previous calculations have shown them to be energetically unfavorable (Li et al., 2005; Zhang and Oganov, 2006), so they are not considered in this paper. Plus, neglecting separated pairs would not affect our analysis of Mössbauer spectra, as the QS of iron in Pv/Ppv is mainly determined by the 3d orbital occupancy and is not sensitive to the neighboring cations. In Fig. 3(a), relative enthalpies (ΔH) of the three considered configurations in the relevant spin states are plotted. Among these configurations, $(\text{Mg,Fe})(\text{Si,Al})\text{O}_3$ with HS Fe^{3+} in the A-site (referred to as “A-HS”) is the most stable one; B-site HS or LS Fe^{3+} in $(\text{Mg,Al})(\text{Si,Fe})\text{O}_3$ (referred to as “B-HS” and “B-LS”) are the least favorable, depending on pressure. However, enthalpies associated with B-site LS Fe^{3+} decrease with pressure, whether in the B-LS state,

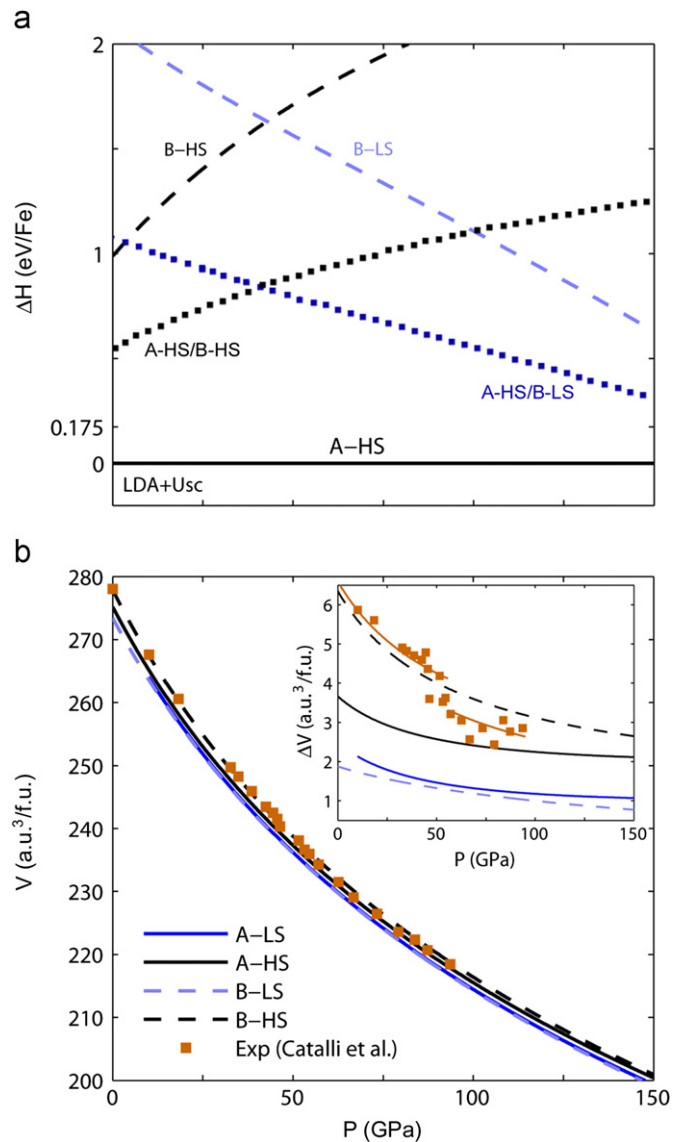


Fig. 3. Relative enthalpies (a) and compression curves (b) of Al-bearing Pv in various atomic configurations. The experimental data in (b) is adopted from Catalli et al. (2011), and the inset shows the volume difference with respect to computed MgSiO_3 compression curve. Solid lines: $(\text{Mg,Fe})(\text{Si,Al})\text{O}_3$; dashed lines: $(\text{Mg,Al})(\text{Si,Fe})\text{O}_3$; dotted lines: mixture of $(\text{Mg,Fe})(\text{Si,Fe})\text{O}_3$ and $(\text{Mg,Al})(\text{Si,Al})\text{O}_3$.

or in the Fe–Fe pair in the mixture of $(\text{Mg,Fe})(\text{Si,Fe})\text{O}_3$ and $(\text{Mg,Al})(\text{Si,Al})\text{O}_3$ with HS Fe^{3+} in the A-site and LS Fe^{3+} in the B-site (referred to as “A-HS/B-LS”). This result suggests that at high pressures and high temperatures, metastable configurations with B-site LS Fe^{3+} can be achieved through diffusion: some of the A-site HS Fe^{3+} migrate to the B-site and become LS Fe^{3+} . Since the sample used by Li et al. (2006) was maintained at room temperature ($k_B T \sim 0.025$ eV) without annealing, the A-site Fe^{3+} barely migrated to the B-site, so the population of B-site Fe^{3+} was too low to be observed. In contrast, Catalli et al. (2011) annealed their sample to ~ 2100 K ($k_B T \sim 0.175$ eV) after each compression, enough to induce some iron migration and accompanying spin change at high pressures (a more quantitative analysis is given below). If the annealed sample is cooled down rapidly, the migrating irons can be trapped in the B-site in the LS state, and be observed in Mössbauer spectra at room temperature. Below 60 GPa, the population of B-site Fe^{3+} is very low (even at high temperature) due to its high enthalpy, so the B-site HS-LS crossover exhibited in Al-free Pv was not observed. Similar annealing-induced iron migration and iron spin change were also observed by Fujino et al. (2012). Based on the above discussion, the emergence of B-site LS Fe^{3+} in experiments is sensitive to the annealing temperature and schedule. The above result also suggests a possible separation of Al-bearing Pv into Al-rich and Fe-rich phases at the high pressures and temperatures of the mantle. This possibility should be carefully investigated by solid-solution calculations and by experiments using sufficiently long annealing times.

The equation of state [Fig. 3(b)] is qualitatively consistent with the above-mentioned scenario. A volume reduction of $\sim 0.3\%$ accompanying the iron migration and spin change is reported by Catalli et al. (2011). This reported volume reduction, as shown in the inset of Fig. 3(b), is about half of the volume difference between the A-HS and B-LS states ($\sim 0.6\%$). Such a result suggests that in the experiment of Catalli et al. (2011), not all, but only a fraction ($\sim 50\%$) of the A-site Fe^{3+} (in the HS state) migrated to B-site (and turned into the LS state) during annealing at high pressures.

We should point out that the fraction of migrating Fe^{3+} predicted by our current calculation in combination with a thermodynamic analysis is lower than that extracted from the above-mentioned volume reduction. Without considering phonon, the molar fraction n_σ of each state (indexed by σ) at any pressure and temperature can be estimated using the following approximation (Hsu et al., 2010c, 2011; Tsuchiya et al., 2006; Wentzcovitch et al., 2009; Wu et al., 2009):

$$n_\sigma \propto m_\sigma (2S_\sigma + 1) \exp(-\Delta H_\sigma / k_B T), \quad (1)$$

subject to the constraint

$$\sum_\sigma n_\sigma = 1, \quad (2)$$

where m_σ and S_σ are the orbital degeneracy and total electron spin of state σ . Here, we only consider the states shown in Fig. 3, namely, σ can only be A-HS, B-HS, B-LS, A-HS/B-HS or A-HS/B-LS. At 100 GPa and 2100 K, one can obtain $n_\sigma \sim 4\%$ for the A-HS/B-LS state, namely, about 4% of the Fe^{3+} occupies the B-site. This estimate is significantly smaller than 50% as suggested by volume reduction. Such a discrepancy is not surprising because not all possible atomic configurations that can occur in a solid solution were considered in our calculations. For example, we did not consider separated pairs or other more complicated Fe–Al clustering that can be investigated only via larger supercells (e.g. a 160-atom supercell containing four Al and four Fe atoms). Based on the result shown in Fig. 3, one can expect that among the configurations that can only be investigated using larger

supercells, the enthalpies of those associated with B-site LS Fe^{3+} should decrease with pressure, just like the A-HS/B-LS and B-LS states in a 40-atom cell. Neglecting these possible configurations (or even other possible unknown atomic structures in the iron-rich region) is a probable cause of underestimating iron migration. In addition, there can be uncertainty in the relative enthalpies [Fig. 3(a)] predicted by DFT+ U_{sc} . Evident from Eq. (1), uncertainty in ΔH_σ directly affects the predicted pressure at which iron migration or the possible phase separation occurs, the amount of iron migration at a given pressure and temperature, and the volume reduction associated with iron migration. Our current calculations, while explaining Mössbauer spectra and the experimental equation of state, are more at a qualitative level. For Al-bearing Pv, many issues still need to be addressed, including element partitioning in the presence of co-existing phases, the resulting Al concentration, and the $\text{Fe}^{3+}/\text{Fe}^{2+}$ population ratio. Since the spin crossover and associated anomalies in Al-bearing Pv are sensitive to these factors, investigation of solid solution behavior at lower mantle conditions is necessary.

3.2. Fe- and Al-bearing MgSiO_3 post-perovskite

To understand how the presence of aluminum affects iron spin state in Al-bearing Ppv, we analyze the response of A- and B-site iron spin state to pressure by considering $(\text{Mg,Fe})(\text{Si,Al})\text{O}_3$ and $(\text{Mg,Al})(\text{Si,Fe})\text{O}_3$ Ppv [see Fig. 1(b)] separately, similar to our analysis for Al-bearing Pv presented in Section 3.1. As shown in Fig. 4, the B-site Fe^{3+} undergoes a HS-LS crossover, but at a pressure where Ppv is a metastable phase (~ 25 GPa), while the A-site Fe^{3+} remains in the HS state in 0–150 GPa. In the D'' pressure range, A- and B-site Fe^{3+} are in the HS and LS state, respectively, same as in Al-free Ppv (Yu et al., 2012).

The substitution mechanism of Fe^{3+} in Al-bearing Ppv and its effect on iron spin state are investigated as well. Similar to Pv (Section 3.1), three distinct configurations are considered: $(\text{Mg,Fe})(\text{Si,Al})\text{O}_3$, $(\text{Mg,Al})(\text{Si,Fe})\text{O}_3$, and a mixture of $(\text{Mg,Fe})(\text{Si,Fe})\text{O}_3$ and $(\text{Mg,Al})(\text{Si,Al})\text{O}_3$ Ppv. Relative enthalpies of these configurations shown in Fig. 5 indicate that in the D'' pressure range, the majority of Fe^{3+} should occupy the A-site and remains in the HS state, and a fraction of Fe^{3+} can occupy the B-site and remains in the LS state at high temperatures. The above result, that Fe^{3+} prefers the A-site in Ppv, is different from a GGA calculation for the end member reported by Caracas (2010), which suggested AlFeO_3 Ppv being more stable than FeAlO_3 Ppv. By comparing Figs. 3 and 5, one can also notice that for Ppv, the enthalpy difference between the most stable configuration (A-HS) and the metastable mixture of $(\text{Mg,Fe})(\text{Si,Fe})\text{O}_3$ and $(\text{Mg,Al})(\text{Si,Al})\text{O}_3$ is smaller than that in Pv, suggesting that Al and Fe are more likely to separate in Ppv, consistent with the previous GGA calculations (Zhang and Oganov, 2006). Nevertheless, spin

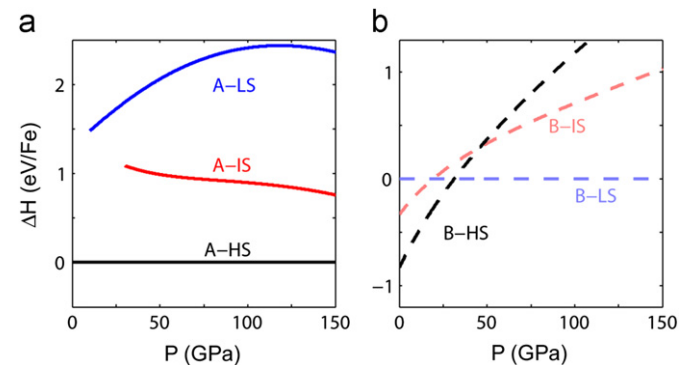


Fig. 4. Relative enthalpies of Al-bearing MgSiO_3 Ppv in different spin states. (a) A-site Fe^{3+} in $(\text{Mg,Fe})(\text{Si,Al})\text{O}_3$ and (b) B-site Fe^{3+} in $(\text{Mg,Al})(\text{Si,Fe})\text{O}_3$.

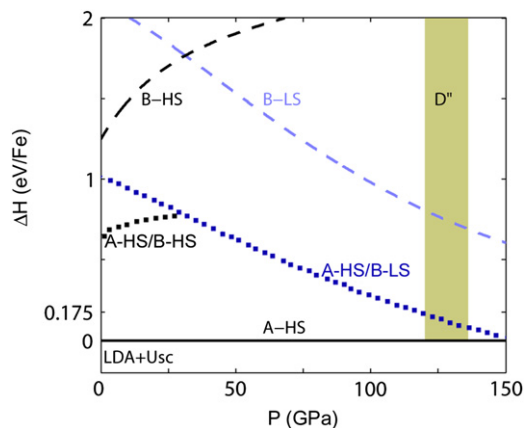


Fig. 5. Relative enthalpies of Al-bearing Ppv in various atomic configurations. Solid line: (Mg,Fe)(Si,Al)O₃; dashed lines: (Mg,Al)(Si,Fe)O₃; dotted lines: mixture of (Mg,Fe)(Si,Fe)O₃ and (Mg,Al)(Si,Al)O₃. The shaded region indicates the D'' pressure range.

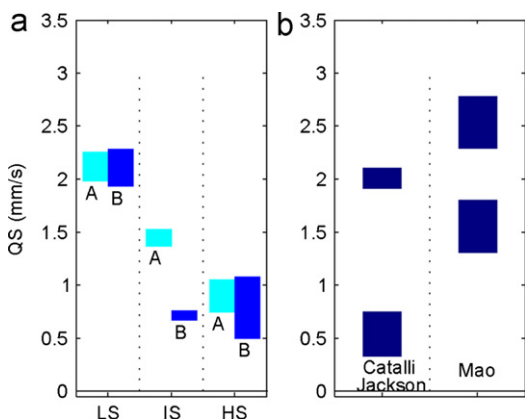


Fig. 6. (a) Computed QSs of iron in all spin states at A- and B-sites. The QSs of B-site HS and IS Fe³⁺ are newly computed; the remaining are adopted from Yu et al. (2012). (b) QS of iron extracted from Mössbauer spectra of Al-free Ppv (Catalli et al., 2010a; Jackson et al., 2009; Mao et al., 2010).

crossover is *not* observed in the D'' pressure range, regardless of the presence or absence of aluminum. The computed QSs shown in Fig. 6 are consistent with those extracted from Al-free Ppv (Mao et al., 2010; Jackson et al., 2009; Catalli et al., 2010a). Further theoretical investigations (solid solution) for Ppv at the D'' condition are desirable as well.

4. Conclusion

Using DFT+*U* calculations, we have investigated the effect of aluminum on the spin crossover of Fe³⁺ in MgSiO₃ perovskite and post-perovskite. We find that the presence of Al³⁺ does not directly change the response of iron spin state to pressure, but it does significantly affect the placement of iron in these mineral phases. For Al-bearing Ppv, the most stable atomic configuration at zero temperature in the 0–150 GPa pressure range has all Fe³⁺ occupying the A-site and being in the HS state; metastable configurations with B-site LS Fe³⁺ can be achieved only at high pressures and high temperatures. Consequently, the pressure-induced B-site HS-LS crossover occurring in Al-free Ppv at 50–60 GPa is not observed in Al-bearing Ppv, due to the low population of B-site Fe³⁺ in this pressure range. On the other hand, a sufficiently high annealing temperature (e.g. 2100 K) can induce a fraction of A-site HS Fe³⁺ to migrate to the B-site at high

pressure (e.g. 80 GPa), accompanied by a change of iron spin state, from HS to LS. If the Pv sample is quenched rapidly, the metastable B-site LS Fe³⁺ can remain trapped and be observed at room temperature. Without annealing, such migration and spin change do not occur. Therefore, the elastic anomalies accompanying the B-site HS-LS crossover exhibited in Al-free Ppv may be considerably reduced in the Earth's lower mantle. As to Al-bearing Ppv, neither A- nor B-site Fe³⁺ undergoes a spin crossover in the D'' pressure range. A-site Fe³⁺ remains in the HS state, and B-site Fe³⁺ remains in the LS state. It should be noted, however, that the uncertainty in the predicted enthalpy differences affect the prediction for the pressure at which iron migration occurs. Further investigations for the equilibrium site occupancies at high pressures and temperatures in Ppv/Ppv are highly desirable, so the volume/elastic anomalies identified in experiments and in the lower mantle can be better clarified.

Acknowledgments

This work was supported primarily by the MRSEC Program of NSF under DMR-0212302 and DMR-0819885 and partially by EAR-081272 and EAR-1047629. Calculations were performed at the Minnesota Supercomputing Institute (MSI).

References

Badro, J., Fiquet, G., Guyot, F., Rueff, J., Struzhkin, V., Vanko, G., Monaco, G., 2003. Iron partitioning in Earth's mantle: toward a deep lower mantle discontinuity. *Science* 300, 789–791.

Badro, J., Rueff, J., Vanko, G., Monaco, G., Fiquet, G., Guyot, F., 2004. Electronic transitions in perovskite: possible nonconvecting layers in the lower mantle. *Science* 305, 383–386.

Bengtson, A., Persson, K., Morgan, D., 2008. *Ab initio* study of the composition dependence of the pressure-induced spin crossover in perovskite (Mg_{1-x}Fe_x)SiO₃. *Earth Planet. Sci. Lett.* 265, 535–545.

Bengtson, A., Li, J., Morgan, D., 2009. Mössbauer modeling to interpret the spin state of iron in (Mg,Fe)SiO₃. *Geophys. Res. Lett.* 36, L15301.

Blaha, P., Schwarz, K., Madsen, G.K.H., Kvasnicka, D., Luitz, J., 2001. WIEN2k, An Augmented Plane Wave + Local Orbitals Program for Calculating Crystal Properties. In: Schwarz, K. (Ed.), *Techn. Universität Wien, Vienna*.

Caracas, R., 2010. Spin and structural transition in AlFeO₃ and FeAlO₃ perovskite and post-perovskite. *Phys. Earth Planet. Inter.* 182, 10–17.

Catalli, K., Shim, S.-H., Prakapenka, V., Zhao, J., Sturhahn, W., 2010a. X-ray diffraction and Mössbauer spectroscopy of Fe³⁺-bearing Mg-silicate post-perovskite at 128–138 GPa. *Am. Mineral.* 95, 418–421.

Catalli, K., Shim, S.-H., Prakapenka, V., Zhao, J., Sturhahn, W., Chow, P., Xiao, Y., Liu, H., Cynn, H., 2010b. Evans W., 2010. Spin state of ferric iron in MgSiO₃ perovskite and its effect on elastic properties. *Earth Planet. Sci. Lett.* 289, 68–75.

Catalli, K., Shim, S.-H., Dera, P., Prakapenka, V., Zhao, J., Sturhahn, W., Chow, P., Xiao, Y., Cynn, H., Evans, W., 2011. Effects of the Fe³⁺ spin transition on the properties of aluminous perovskite—new insights for lower-mantle seismic heterogeneities. *Earth Planet. Sci. Lett.* 310, 293–302.

Cococcioni, M., 2010. Accurate and efficient calculations on strongly correlated minerals with the LDA plus *U* method: review and perspectives. *Rev. Mineral Geochem.* 71, 147–167.

Cococcioni, M., de Gironcoli, S., 2005. Linear response approach to the calculation of the effective interaction parameters in the LDA + *U* method. *Phys. Rev. B* 71, 035105.

Crowhurst, J., Brown, J., Goncharov, A., Jacobsen, S., 2008. Elasticity of (Mg,Fe)O through the spin transition of iron in the lower mantle. *Science* 319, 451–453.

Dudarev, S.L., Botton, G.A., Savrasov, S.Y., Humphreys, C.J., Sutton, A.P., 1998. Electron-energy-loss spectra and the structural stability of nickel oxide: an LSDA+*U* study. *Phys. Rev. B* 57, 1505–1509.

Frost, D.J., Liebske, C., Langenhorst, F., McCammon, C.A., Tronnes, R.G., Rubie, D.C., 2004. Experimental evidence for the existence of iron-rich mineral in the Earth's lower mantle. *Nature* 428, 409–412.

Fujino, K., Nishio-Hamane, D., Seto, Y., Sata, N., Nagai, T., Shinmei, T., Irifune, T., Ishii, H., Hiraoka, N., Cai, Y., Tsue, K.-D., 2012. Spin transition of ferric iron in Al-bearing Mg perovskite up to 200 GPa and its implication for the lower mantle. *Earth Planet. Sci. Lett.* 317–318, 407–412.

Giannozzi, P., Baroni, S., Bonini, N., Calandra, M., Car, R., Cavazzoni, C., Ceresoli, D., Chiarotti, G.L., Cococcioni, M., Dabo, I., Dal Corso, A., de Gironcoli, S., Fabris, S., Fratesi, G., Gebauer, R., Gerstmann, U., Gougoussis, C., Kokalj, A., Lazzeri, M., Martin-Samos, L., Marzari, N., Mauri, F., Mazzarello, R., Paolini, S., Pasquarello, A., Paulatto, L., Sbraccia, C., Scandolo, S., Sclauzero, G., Seitsonen, A.P., Smogunov, A., Umari, P., Wentzcovitch, R.M., 2009. QUANTUM ESPRESSO: a

- modular and open-source software project for quantum simulations of materials. *J. Phys.: Condens. Matter* 21, 395502.
- Goncharov, A., Struzhkin, V., Jacobsen, S., 2006. Reduced radiative conductivity of low-spin (Mg,Fe)O in the lower mantle. *Science* 312, 1205–1208.
- Hofmeister, A.M., 2006. Is low-spin Fe²⁺ present in Earth's mantle? *Earth Planet. Sci. Lett.* 243, 44–52.
- Hsu, H., Blaha, P., Cococcioni, M., Wentzcovitch, R.M., 2011. Spin-state crossover and hyperfine interactions of ferric iron in MgSiO₃ perovskite. *Phys. Rev. Lett.* 106, 118501.
- Hsu, H., Blaha, P., Wentzcovitch, R.M., 2012. Ferromagnetic insulating state in tensile-strained LaCoO₃ thin film from LDA+ *U* calculations. *Phys. Rev. B* 85, 140404(R).
- Hsu, H., Blaha, P., Wentzcovitch, R.M., Leighton, C., 2010a. Cobalt spin states and hyperfine interactions in LaCoO₃ investigated by LDA+ *U* calculations. *Phys. Rev. B* 82, 100406(R).
- Hsu, H., Umemoto, K., Blaha, P., Wentzcovitch, R.M., 2010b. Spin states and hyperfine interactions of iron in (Mg,Fe)SiO₃ perovskite under pressure. *Earth Planet. Sci. Lett.* 294, 19–26.
- Hsu, H., Umemoto, K., Wu, Z., Wentzcovitch, R.M., 2010c. Spin-state crossover of iron in lower-mantle minerals: results of DFT+*U* investigations. *Rev. Mineral Geochem.* 71, 169–199.
- Irfune, T., 1997. Absence of an aluminous phase in the upper part of the Earth's lower mantle. *Nature* 370, 131–133.
- Jackson, J.M., Sturhahn, W., Shen, G., Zhao, J., Hu, M.Y., Errandonea, D., Bass, J.D., Fei, Y., 2005. A synchrotron Mössbauer spectroscopy study of (Mg,Fe)SiO₃ perovskite up to 120 GPa. *Am. Mineral.* 90, 199–205.
- Jackson, J.M., Sturhahn, W., Tschauner, O., Lerche, M., Fei, Y., 2009. Behavior of iron in (Mg,Fe)SiO₃ post-perovskite assemblages at Mbar pressures. *Geophys. Res. Lett.* 36, L10301.
- Kesson, S.E., Fitz gerald, J.D., Shelley, J.M., 1998. Mineralogy and dynamics of a pyrolite lower mantle. *Nature* 393, 252–255.
- Kulik, H., Cococcioni, M., Scherlis, D.A., Marzari, N., 2006. Density functional theory in transition metal chemistry: a self-consistent Hubbard *U* approach. *Phys. Rev. Lett.* 97, 103001.
- Li, J., Struzhkin, V., Mao, H., Shu, J., Memeley, R., Fei, Y., Mysen, B., Dera, P., Pralapenka, V., Shen, G., 2004. Electronic spin state of iron in lower mantle perovskite. *Proc. Natl. Acad. Sci.* 101, 14027–14030.
- Li, J., Sturhahn, W., Jackson, J.M., Struzhkin, V.V., Lin, J.F., Zhao, J., Mao, H., Shen, G., 2006. Pressure effect on the electronic structure of iron in (Mg,Fe)(Si,Al)O₃ perovskite: a combined synchrotron Mössbauer and X-ray emission spectroscopy study up to 100 GPa. *Phys. Chem. Minerals.* 33, 575–585.
- Li, L., Brodholt, J., Stackhouse, S., Weidner, D., Alfredsson, M., Price, G., 2005. Electronic spin-state of ferric iron in Al-bearing perovskite in the lower mantle. *Geophys. Res. Lett.* 32, L17307.
- Lin, J.-F., Struzhkin, V., Jacobsen, S., Hu, M., Chow, P., Kung, J., Liu, H., Mao, H., Hemley, R., 2005. Spin transition of iron in magnesiowüstite in the Earth's lower mantle. *Nature* 436, 377–380.
- Lin, J.-F., Vanko, G., Jacobsen, S., Iota, V., Struzhkin, V., Prakapenka, V., Kuznetsov, A., Yoo, C., 2007a. Spin transition zone in the Earth's lower mantle. *Science* 317, 1740–1743.
- Lin, J.-F., Weir, S.T., Jackson, D.D., Evans, W.J., Vohra, Y.K., Qiu, W., Yoo, C.-S., 2007b. Electrical conductivity of the lower-mantle ferropericlae across the electronic spin transition. *Geophys. Res. Lett.* 34, L16305.
- Lin, J.-F., Watson, H., Vanko, G., Alp, E.E., Prakapenka, V.B., Dera, P., Struzhkin, V., Kubo, A., Zhao, J., McCammon, C., Evans, W.J., 2008. Intermediate-spin ferrous iron in lowermost mantle post-perovskite and perovskite. *Nature Geosci.* 1, 688–691.
- Lin, J.-F., Alp, E.E., Mao, Z., Inoue, T., McCammon, C., Xiao, Y., Chow, J., 2012. Electronic spin states of ferric and ferrous iron in the lower-mantle silicate perovskite. *Am. Mineral.* 97, 592–597.
- Madsen, G., Blaha, P., Schwarz, K., Sjoestedt, E., Nordstroem, L., 2001. Efficient linearization of the augmented plane-wave method. *Phys. Rev. B* 64, 195134.
- Mao, Z., Lin, J.-F., Jacpbs, C., Watson, H., Xiao, Y., Chow, P., Alp, E., Prakapenka, V., 2010. Electronic spin and valence state of Fe in CaIrO₃-type silicate post-perovskite in the Earth's lowermost mantle. *Geophys. Res. Lett.* 37, L22304.
- McCammon, C., 1997. Perovskite as a possible sink for ferric iron in the lower mantle. *Nature* 387, 694–696.
- McCammon, C., Kantor, I., Narigina, O., Rouquette, J., Ponkratz, U., Sergueev, I., Mezouar, M., Prakapenka, V., Dubrovinsky, L., 2008. Stable intermediate-spin ferrous iron in lower-mantle perovskite. *Nature Geosci.* 1, 684–687.
- Perdew, J.P., Burke, K., Ernzerhof, M., 1996. Generalized gradient approximation made simple. *Phys. Rev. Lett.* 77, 3865–3868.
- Petrilli, H.M., Blöchl, P.E., Blaha, P., Schwarz, K., 1998. Electric-field-gradient calculations using the projector augmented wave method. *Phys. Rev. B* 57, 14690–14697, and references therein.
- Stackhouse, S., Brodolt, J.P., Price, G.D., 2007. Electronic spin transitions in iron-bearing MgSiO₃ perovskite. *Earth Planet. Sci. Lett.* 253, 282–290.
- Tsuchiya, T., Wentzcovitch, R.M., de Silva, C.R.S., de Gironcoli, S., 2006. Spin transition in magnesiowüstite in Earth's lower mantle. *Phys. Rev. Lett.* 96, 198501.
- Umemoto, K., Wentzcovitch, R., Yu, Y., Requist, R., 2008. Spin transition in (Mg,Fe)SiO₃ perovskite under pressure. *Earth Planet. Sci. Lett.* 276, 198–206.
- Umemoto, K., Hsu, H., Wentzcovitch, R.M., 2009. Effect of site degeneracies on the spin crossovers in (Mg,Fe)SiO₃ perovskite. *Phys. Earth Planet. Inter.* 180, 209.
- Wentzcovitch, R., Martins, J.L., Price, G.D., 1993. *Ab initio* molecular dynamics with variable cell shape: application to MgSiO₃. *Phys. Rev. Lett.* 70, 3947–3950.
- Wentzcovitch, R.M., Justo, J., Wu, Z., da Silva, C.R.S., Yuen, D., Kohlstedt, D., 2009. Anomalous compressibility of ferropericlae throughout the iron spin crossover. *Proc. Natl. Acad. Sci. USA* 106, 8447–8452.
- Wu, Z., Justo, J., da Silva, C.R.S., de Gironcoli, S., Wentzcovitch, R.M., 2009. Anomalous thermodynamic properties in ferropericlae throughout its spin crossover transition. *Phys. Rev. B* 80, 014409.
- Yu, Y., Hsu, H., Cococcioni, M., Wentzcovitch, R.M., 2012. Spin-states and hyperfine interactions of iron incorporated in MgSiO₃ post-perovskite. *Earth Planet. Sci. Lett.* 331–332, 1–7.
- Zhang, F., Oganov, A.R., 2006. Valence state and spin transitions of iron in Earth's mantle silicates. *Earth Planet. Sci. Lett.* 249, 436–443.